A simple descriptor for energetics at fcc-bcc metal interfaces[☆]

Linda A. Zotti^{1,2}, Stefano Sanvito², David D. O'Regan²

¹Departamento de Física Teorica de la Materia Condensada, Universidad Autónoma de Madrid, 28049 Madrid, Spain

²School of Physics, AMBER and CRANN Institute, Trinity College Dublin, Dublin 2, Ireland

Abstract

We have developed a new and user-friendly interface energy calculation method that avoids problems deriving from numerical differences between bulk and slab calculations, such as the number of k points along the direction perpendicular to the interface. We have applied this to 36 bcc-fcc metal interfaces in the (100) orientation and found a clear dependence of the interface energy on the difference between the work functions of the two metals, on the one hand, and the total number of d electrons on the other. Greater mechanical deformations were observed in fcc crystals than in their bcc counterparts. For each bcc metal, the interface energy was found to follow the position of its d band, whereas the same was not observed for fcc.

Keywords: Metallic interfaces, interface energy, work of separation, ab initio simulations, surface energy

1. Introduction

The study of metal-metal interfaces is crucial for many industrial processes and technological applications [1–3], including growth modes in thin films [4, 5], catalysis [6], as well as many experimental techniques used in nanotechnology such as those involving metallic tips on metal surfaces [7]. Theoretical support in designing metallic interfaces is essential as it can provide information that is extremely difficult to extract experimentally. An example is given by interface energies, which determine the nucleation barrier and the shapes of precipitates [8–10], besides the stability and reliability of the whole system. These energies are not directly accessible experimentally. Thorough studies have been performed at the level of first-principles calculations on selected solid-solid interfaces, focusing on various aspects such as the film thickness [4], orientation [7], magnetoresistance [11], magnetic anisotropy [12] ferromagnetic moments [13], as well as electronic [14–17], mechanical [18–21], and thermodynamic [22–26] properties. Notwithstanding the detailed nature of these analyses, they were

In particular, we aimed to understand whether it is possible to predict trends in interface energetics on the basis of simple bulk properties. In previous work, on the basis of non-first-principles calculations [27], interface energies were found to depend on the balance between several quantities, including the number of d electrons per atom in the interface layers and in the bulk, the bandwidth of the interface layers and the bulk, the cohesive energies, the Fermi levels and the intra-atomic potentials. We show here, instead, that modern density functional

 $Email\ address:$ linda.zotti@uam.es (Linda A. Zotti 1,2)

quite often mostly focused on a very few materials. What is currently still missing is, for instance, a systematic analysis and a rule of thumb as to how to "cherry pick" materials and match them, ensuring stability of their interface at the same time. In this work, therefore, we chose to follow a different approach. We focused on only one crystal orientation (100) and on one type of relative dislocation between the two metals, but we performed a systematic analysis spanning over 36 interfaces. These were obtained by combining 6 face-centeredcubic (fcc) crystals (Au, Ag, Cu, Ni, Pd, Pt) with 6 body-centered-cubic (bcc) crystals (Cr, Mo, W, Nb, V, Ta). Such an approach has allowed us to formulate a descriptor for interface energies based on very similar conditions for all systems.

 $^{^{\}circ}$ Manuscript accepted on $10^{\rm th}$ January 2018 and published as 'Linda A. Zotti, Stefano Sanvito, and David D. O'Regan, Materials and Design **142** (2018) 158165', for which see https://doi.org/10.1016/j.matdes.2018.01.019

 $[\]textcircled{c} \ \ 2018. \ \ This is made available under the \ CC-BY-NC-ND \ 4.0 \ license, \ http://creativecommons.org/licenses/by-nc-nd/4.0/ \ . \\$

theory (DFT) calculations make it possible to reveal much simpler relationships. In particular, we show that, for certain metal pairs, simply the difference between their work functions or the sum of the electrons in their d bands can provide a first hint on the stability of the interface. We anticipate that this will prove to be a very useful finding for the design of metallic multi-layers and heterostructures for technological applications. Our work is particularly timely and relevant for interface layer selection and design in the context of high-throughput materials simulation and informatics, a research area which is gaining increasing traction at present.

2. Methods

The interface energy is the energy cost associated with the introduction of an interface. It can be interpreted as the surface "binding" energy density of the two components. It comprises two contributions, namely the chemical and electronic energy that originates from breaking and creating bonds to form an interface, and the elastic energy required to create the interface by matching the two lattices [28]. We mainly focus on the electronic component and neglect the elastic contribution, which goes beyond the scope of the present work. Within one of the most accurate methods to date [29], the interface energy γ can be calculated as:

$$\gamma = E'_{\text{fcc/bcc}} - E^{\text{bulk}}_{\text{fcc}} - E^{\text{bulk}}_{\text{bcc}}, \tag{1}$$

where

$$E'_{\text{fcc/bcc}} = E_{\text{fcc/bcc}} - \sigma_{\text{fcc}} - \sigma_{\text{bcc}}.$$
 (2)

Here, $E_{\rm fcc/bcc}$ is the total energy of the system, $E_{\rm x}^{\rm bulk}$ is the total energy of the crystal in the bulk state. The surface energies $\sigma_{\rm x}$ are calculated relative to the bulk crystal experiencing the same strain as in the interface (see Ref. [29] for details), via

$$\sigma_{\rm x} = (E_{\rm x} - E_{\rm x}^{\rm bulk})/2. \tag{3}$$

Although this method has proven successful [29], it requires five separate calculations (one for the interface, two for the corresponding bulk materials and two for their free surfaces), which require particular care when defining the unit-cell dimensions and the corresponding strain in each of them. More importantly, it carries the intrinsic problem of performing algebraic operations between quantities that are calculated using different numbers of k

points. In fact, the lattice periodicity is preserved in all three space directions in bulk crystals, but only in two directions at surfaces. Consequently, energies computed for bulk and slab calculations are not directly comparable for all thickness values and slow convergence of the calculated interface energy with respect to the number of layers can thereby arise. Slight variations of Eq. 1 have also been used [30], but these present the same problem.

We thus propose an alternative method, namely an extension of the Fiorentini procedure [31] that was originally developed to calculate surface energies, and which has been shown to provide accelerated convergence with respect to the number of layers in the system [32]. Surface energy is the energy needed to cleave a bulk crystal into two separate surfaces [4] and it can be expressed as

$$\sigma = \lim_{N \to \infty} \frac{1}{2} (E_N^{\text{slab}} - N E^{\text{bulk}}), \tag{4}$$

where $\mathbf{E}_N^{\mathrm{slab}}$ is the total energy of an N-atom slab and $\mathbf{E}_{\mathrm{bulk}}$ is the total energy of the bulk per atom. Within the Fiorentini method, $\mathbf{E}_{\mathrm{bulk}}$ can be calculated as the slope in $\mathbf{E}_N^{\mathrm{slab}}$ plotted against N and then used in equation 4. This is possible because the following linear relationship applies:

$$E_N^{\rm slab} \approx 2\sigma + N E^{\rm bulk}$$
. (5)

This method allows us to avoid problems deriving from calculating $\mathbf{E}_N^{\mathrm{slab}}$ and $\mathbf{E}^{\mathrm{bulk}}$ with a different number of k points. We note that, if one-atom unit cells are considered, N equals the number of layers.

By replacing the vacuum region with another metal, we have extended this scheme to the calculation of interface energies. In fact, in the same way that interface energies are the energies originating from breaking old bonds and creating new bonds in the interface, surface energies can likewise be interpreted as the energy involved in breaking the same old bonds and creating new "bonds" with the vacuum. Within such a scheme, we built, for each fccbcc interface, at least three structures which differ from each other by the number of layers on each side (see Fig. 1). After collecting the total energies of each structure, we extracted the slope s of the total energy of the fcc-bcc system $E_{N_x+N_y}$ versus the total number of layers N_x+N_y , where N_x and Ny are the number of layers on each side of the interface. The interface energy γ is then given by

$$\gamma = (E_{N_{x}+N_{y}} - (N_{x} + N_{y}) * s)/2, \tag{6}$$

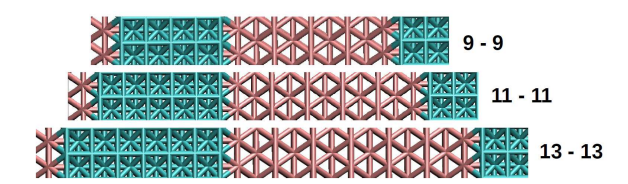


Figure 1: Examples of slabs with different numbers of layers in both fcc and bcc metals (indicated on the right hand side) as used in our extended "Fiorentini" approach for interfaces.

where $E_{N_x+N_y}$ and N_x+N_y must be taken from the same structure. As for surface energies, this method avoids problems arising due to numerical differences between bulk and slab calculations for interface energies. In addition, it only requires two simple calculations (although it is recommendable to perform at least one more to make sure the slope is evaluated in the linear regime). The work of separation W (the energy needed to separate the interface into two free surfaces) is given by [1, 33]

$$W = \sigma_{\rm fcc} + \sigma_{\rm bcc} - \gamma. \tag{7}$$

In order to calculate the necessary total energies, we carried out density functional theory (DFT) calculations by using the PWscf code of the Quantum ESPRESSO distribution [34], which uses a planewave basis. The LDA exchange-correlation functional was used, with a kinetic energy cutoff for wave-functions of 50 Ry and, for the charge density and potential, of 400 Ry. This functional was chosen because it has been found to yield better agreement with experiments for surface energies as compared to GGA [32] and because it is known to provide a very good description of structural and energetic properties of solids [35]. For the Brillouinzone integration, we use a Monkhorst-Pack [36] set. Specifically, we used a 16x16x16 k-point grid for bulk calculations, while we used a 16x16x1 sampling for surface calculations. A Fermi-Dirac smearing with a broadening of 0.0038 Ryd ($\approx 600 \text{ K}$) was adopted. Ultrasoft pseudopotentials USPPs [37] were used for all elements. Although some of the systems analyzed are known to present interesting magnetic properties (for example, see Ref. [38]), we forced all systems to be non-magnetic in order to keep their conditions as similar as possible and thus to better isolate the over-arching descriptors for adhesion.

We considered fcc(100)-bcc(100) interfaces consisting of the same number N of layers in each

metal. Periodicity was applied in all three spatial directions. In order to meet this condition, odd values were chosen for N, namely N=9,11,13. For each metal, a slab in contact with a vacuum region of approximately 16 Å on each side was also built in order to calculate surface energies (for this kind of calculation, it does not matter whether an even or odd number of layers is used). To calculate surface energies, the size of the simulation cell was determined using optimized bulk lattice parameters and all atomic coordinates were then relaxed. For the interface energies, instead, cell dimensions were optimized in all three Cartesian directions to ensure a minimal strain induced by the lattice mismatch at the interface.

We emphasise that our surface energies and interface energies were calculated using Eqs. 4-5 and 6, respectively. For selected cases, Eqs. 1-2 were also used for the purposes of comparison (see Table 2).

The (100) faces of the fcc and bcc metal were rotated by 45 degrees with respect to each other in order to provide an optimal match between the bcc lattice constant a_{bcc} and half a diagonal of the fcc face ($a_{fcc}/\sqrt{2}$, a_{fcc} being the fcc lattice constant) [11]. We considered one-atom unit cells, suppressing, therefore, reconstruction effects and long-ranged mismatch. In the 100 orientation, both the bcc and fcc metals present an abab layer stacking. At the interface, the two materials were joined so that the atoms of one metal rested on top of the hollow sites of the other.

3. Results and Discussion

In the colour-coded areas of panel (a) and (b) of Table 1, we report the interface and work of separation calculated by using Eqs. 6 and 7, respectively. The "Vacuum" row and column in panel (a) refer to each individual metal interfaced with vacuum: this is nothing but the surface energy as pointed out above (note that, for Au, the calculated value is in very good agreement with that reported in [32], where the same code and functional were used). All corresponding values in J/nm^2 are shown in Table S1 of the Supporting Information. We can observe that the interface energies shown in panel (a) range from negative to positive values, which corresponds to more and less stable interfaces, respectively.

Before analyzing these results in depth, it is worth comparing some of our values with those that we would obtain by the method described in Eq. 1 and in Ref. [29]. For this purpose, we chose

	Interface energies							
(a)	Cu	Ag	Au	Ni	Pd	Pt	Vacuum	
Cr	0.71	0.84	0.59	-0.04	0.04	-0.11	1.98	
Мо	0.59	0.91	0.52	-0.19	-0.07	-0.58	2.22	
W	0.65	1.20	0.78	-0.29	-0.03	-0.42	2.76	
V	-0.09	0.19	-0.29	-0.58	-0.64	-0.82	1.50	
Nb	0.1	0.52	-0.48	-0.6	-1.01	-1.26	1.79	
Ta	-0.18	0.47	-0.44	-1.02	2 -1.07	-1.32	1.90	
Vacuum	0.80	0.65	0.78	1.08	3 1.01	1.14		
Adhesion energies								
(b)	Cu	Ag	Au	Ni	Pd	Pt		
Cr	2.07	1.79	2.17	3.1	2.95	3.23		
Mo	2.43	1.96	2.48	3.49	3.3	3.94		
w	2.91	2.21	2.76	4.13	3.8	4.32		
V	2.39	1.96	2.57	3.16	3.15	3.46		
Nb	2.49	1.92	3.05	3.47	3.81	4.19		
Ta	2.88	2.08	3.12	4.00	3.98	4.36		

Table 1: (a) Interface energies γ and (b) Work of separation W. All values are given in eV/atom.

one interface with a positive (Ag-W) and one with a negative (Au-Nb) interface energy. In order to apply this method, the fcc-bcc interface was embedded in vacuum. All fcc (bcc) slabs contained an even number of layers, 12, so that the abab stacking was preserved in the corresponding bulk calculations, in which the fcc (bcc) block is repeated periodically in all three spatial directions. In the bulk and surface calculations, the same lateral strain as results in the interface calculation was imposed. The same exchange-correlation functional, pseudopotentials and parameters were used as in the calculations performed according to Eq. 6 and reported in Table 1. All calculated quantities used in the comparison for each system are reported in Table 2. An interface energy difference of 0.03 eV and 0.11 eV was calculated for W-Ag and Nb-Au, respectively, a discrepancy which should ultimately vanish in the limit of large layer number N.

We furthermore calculated the interface energy for a Ag-Fe system in the same orientation and found a value (1.07 J/m^2) that is in very good agreement with those reported for the same interface in Ref. [29]. Although the two methods give comparable results when the recipe described in Eq. 1 is carefully applied, the procedure proposed here is easier to follow and requires fewer types of calculations. It can also be used for interfaces involving materials with different crystal structures, provided that care is taken when defining the number of atoms per unit cell and the number of layers (chosen to enforce periodicity at the boundaries).

Each of Table 1 (a) and (b) is divided into four blocks in order to highlight elements coming from different rows of the periodic table. Specifically, V, Nb and Ta belong to the 3rd column of the transition-metal block; Cr, Mo and W belong to 4th column of the same block; Ni, Pd and Pt belong to the 8th column; and Cu, Ag and Au belong to the 9th column. These specific columns were chosen because, within each of them, the crystal structure is the same across three consecutive rows of the periodic table. The same does not apply instead, for instance, to the 5th to 7th columns, where a mixture of fcc, bcc and hcp structures is present. We anticipate that our qualitative findings will extend to other metal-metal interfaces structures across the periodic table, provided that lattice mismatch, long-range reorganisation, magnetism, or more exotic many-body effects are absent or negligible.

To make it easier for the reader to identify interfaces with similar values of interface energy and work of separation, we varied the cell colours in panel (a) from red (lowest negative values) to blue (highest positive values) and in panel (b) from yellow (lowest positive) to orange (highest positive). The colour-coded areas in panel (a) highlight a tendency towards positive interface energies for the 4th-9th column combinations, and towards negative interface energies for the 3rd-8th column combinations. The sign of the interface energy plays an important role in inter-diffusion and interface stability [39]. Negative values indicate a greater stability of the interface. For the work of separation W, all calculated values are positive but the color-coded areas show a similar color modulation as for the interface energies. To get an insight into the variation observed for these quantities, we investigated possible dependencies on bulk properties, with the aim of developing an approach to optimise adhesion based only on inputs from bulk (high-throughput compatible) calculations.

In panel (a) of Fig. 2, we show the interface energies against (black dots) the sum of the d-band occupation N^d in the two metals (we focussed on this angular momentum because it is known to play a dominant role in binding strength for transition metals [40, 41]). This occupation was evaluated using a separate bulk unit-cell calculation, integrating the d band density of states up to the Fermi energy. A linear trend can be observed, showing negative energies for lower values of the sum and positive in the opposite case. In the same panel we also report (red squares) the interface-energy values as a func-

		Method of Ref. [29]					Proposed method						
	$\text{bulk}_{\mathbf{fcc}}$	bulk _{bcc}	$surface_{fcc}$	$surface_{bcc}$	$E_{\text{fcc/bcc}}$	γ (Ry)	$\gamma \; (\mathrm{eV})$	E(9-9)	E(11-11)	E(13-13)	s	γ (Ry)	$\gamma \; ({ m eV})$
Ag-W Au-Nb	-3548.50 -1378.99	-1910.83 -1417.12	-3548.38 -1378.84	-1910.43 -1416.86	-5458.98 -2795.93	0.09	1.23	-4094.32 -2097.14	-5004.21 -2563.16	-5914.10 -3029.17	-227.47 -116.50	0.09	1.20

Table 2: Interface energies calculated, for selected interfaces, using the method described in Ref. [29] and that which we propose, together with all values of the quantities employed in both. Where not specified, values are expressed in Rydberg. $E_{\rm fcc/bcc}$ is the energy of the fcc-bcc interface embedded in vacuum, bulk_x is the energy of the two bulk metals, surface_x is the energy of the free surface; $E(N_{\rm fcc}-N_{\rm bcc})$ is the energy of a system consisting of an N-layer fcc slab and an N-layer bcc slab as shown in Fig. 1, s is the slope of $N_{\rm fcc}-N_{\rm bcc}$ versus $N_{\rm fcc}+N_{\rm bcc}$, and γ is the interface energy.

tion of the difference between the work functions of the two elements forming the junction. Work functions were calculated as

$$\Phi = V_{\text{Vacuum}} - E_{\text{Fermi}}, \tag{8}$$

where V_{Vacuum} is the vacuum potential and E_{Fermi} is the Fermi energy (see Fig. S1 in the Supporting Information). Both quantities were extracted from calculations performed on the same slabs that were used to compute surface energies. For the metals studied in this work, work functions were generally found to be larger for fcc metals than for bcc ones (see Table 3 for values).

	Work function (eV)	N^d
Ag	4.720	9.54717
Au	5.470	9.48133
Cr	4.394	4.75568
Cu	4.930	9.24695
Mo	4.219	4.73858
Nb	3.873	4.00027
Ni	5.399	8.35574
Pd	5.549	8.8055
Pt	5.783	8.48978
Ta	4.090	3.73651
V	4.054	4.02202
W	4.434	4.54067

Table 3: Work functions and number of d electrons per unit cell for each metal considered.

The behaviour of interface energies versus the difference between work functions shows a linear trend as well, assigning the highest interface energies to the smallest work-function differences. A rather approximate linear trend is also observed with respect to differences between the experimental electronegativity values (see Fig. S2). The linearity of both trends in panel (a) of Fig. 2 derives from work functions and number of d electrons N^d being related, as it can be observed in panel (b) of the same figure.

For the metals here considered, the work function of fcc is larger than that of bcc in all cases. However, the two sets show approximately linear dependences on the number of d electrons with slopes of opposite signs (negative for fcc and positive for bcc): the combination of these two conditions leads to the difference between the two work functions being lower for higher values of N^d in both metals (corresponding, in turn, to higher values of their sum, inset of panel (b)). Note that this cannot be extended to all metals generally. It does not apply, for instance, to interfaces including Fe (bcc), the work function of which is larger than that of some of the fcc metals considered here. It is also worth stressing that our calculations do not include magnetic effects, which could be present in some of the interfaces considered. For instance, it has been found that the Cr atoms of a flat Cr monolayer buried under a layer of Ag atoms retain a significant spin moment [38]. Nevertheless, we chose not to include magnetism in our study in order to compare all interfaces similar conditions, avoiding where possible additional effects which might not occur to the same extent in all materials. Magnetism should, however, be taken into account in a second step to obtain the whole picture, which goes beyond the scope of the present work.

Within the analogy between metal-metal interfaces and metal-vacuum interfaces we also observed (see panel (c)) a dependence on the work function for the surface energies, with two distinct linear trends for the fcc and the bcc set, the slope of the bcc set being higher. The bcc crystals generally presented a higher surface energy than the fcc ones. This is not surprising, given that a higher density of broken bonds yields to a higher surface energy [42]. Within each set, work functions were found to increase for decreasing surface energies, as expected [43]. From Table 1, it can be observed that the lowest interface energies in panel (a) corre-

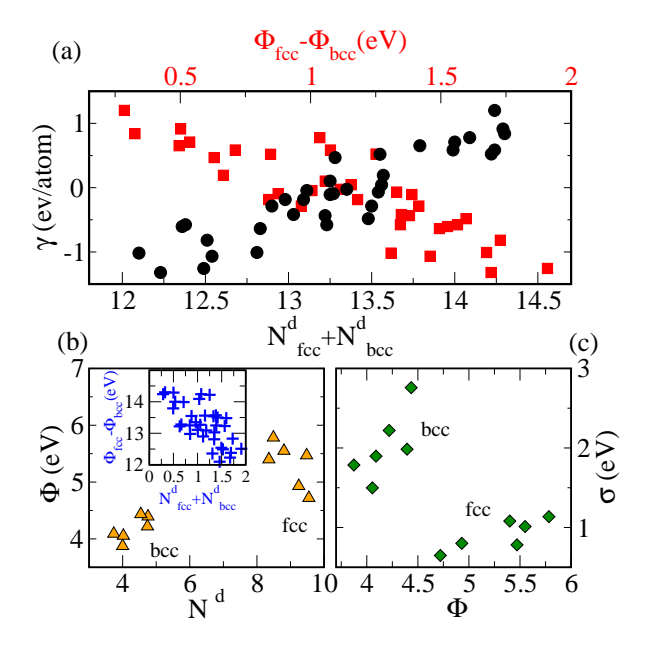


Figure 2: (a) interface energy as a function of the sum of the total number of d electrons N^d (black dots) and as a function of the difference between the bulk Fermi energies of the fcc and bcc metal (red squares); (b) work function as a function of N^d and (inset) difference of work functions versus sum of N^d in the two metals; (c) surface energies as a function of work function.

spond to highest work of separation W in panel (b). In fact, a dependence on the sum of the d occupations and on the difference between work functions was also found for W (Fig. 3), but with opposite signs. Our results can be interpreted as follows: when the work functions of two metals are quite different from each other, charge transfer takes place from fcc to bcc metals with a consequent realignment of their Fermi levels and formation of interface dipoles. Overall, the ensuing electrostatic balance contributes to the stabilization of the interface, and this gives rise to a larger work of separation needed to reestablish the initial situation than if the two work functions were initially closer in value.

Inspired by Norskov's d-band model [40], according to which the bond between a molecule and a metal depends on the position of the d band with respect to the Fermi level, we analyzed the position of the LDA Kohn-Sham d band (using pseudoatomic projection) in the atom of the bcc crystal at the interface when approaching each of the fcc metals considered. This was evaluated as the energetic position of the center of mass of the occupied part of the band with respect to the global Fermi energy of

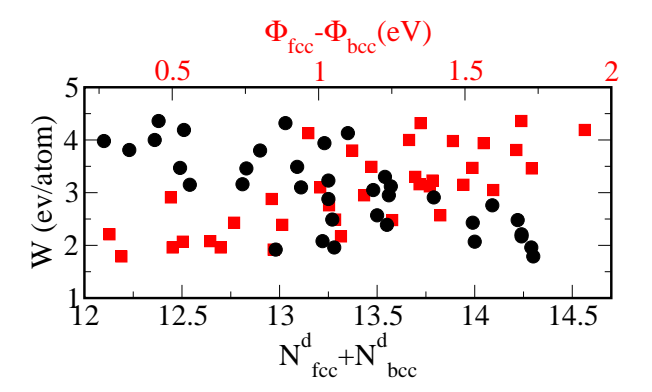


Figure 3: Work of separation W as a function of the sum of d electrons (black dots) and difference of work functions (red squares)

each interface. For this analysis, we used structures consisting of 13 layers on each side of the interface. Interface energies as a function of the so-calculated d-band shifts are shown in Fig. 4 for W, Nb and V in panel (a) as examples. An approximately linear behaviour is visible for them all, with the position of the bcc d band center of mass moving down in energy as the work function of the fcc metal counterpart increases. No clear trend was observed in the opposite case (see panel (b) of the same figure, with Au, Ag and Pt as examples), i.e., referring to the energetic position of the d band in the fcc atom at the interface with each of the six bcc crystals.

For further insight, we analyzed the pseudoatomic Löwdin charges across the junctions for the same systems as in Fig. 4. Such charges are shown for the W, V and Nb atoms in Fig. 5. In all cases, the population at the bcc atom at the interface decreases as the work function of the fcc metal increases (as expected with increasingly favourable conditions for charge transfer from bcc to fcc). The same kind of analysis does not show, however, a clear trend for the fcc metals (see Fig. 6; for Pt, the complete charge profile across the whole junction is shown in Fig. S3 of the Supporting Information). As an aside, we observed a general tendency of the bcc metal to present charge oscillations across the junction more than in the fcc metal.

Overall, our calculated charge distributions show that only the atoms in one or two layers close to the interface are strongly affected by the contact with the other metal. In Fig. 7 we compare, in Ag (fcc) and W (bcc) as examples, the profile of the d band in the atom at the very interface (solid

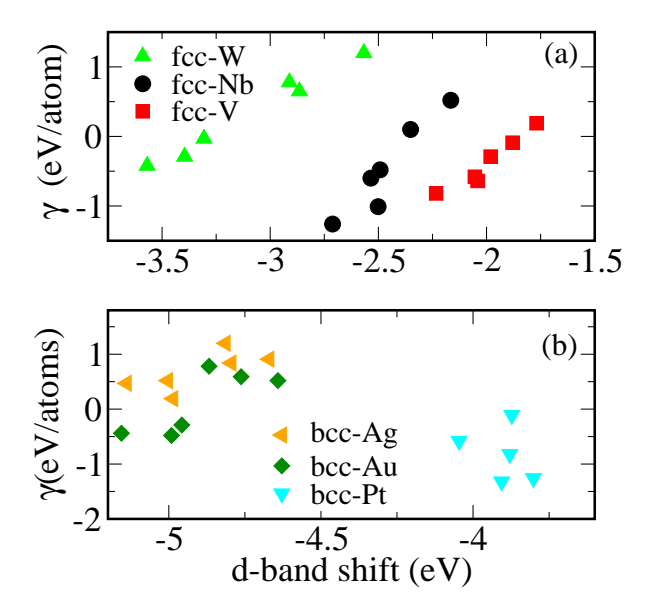


Figure 4: Interface energy as a function of the energy distance of the center of mass of the d band from the common Fermi level in the W, Nb and V atoms at the interface when combined with each of the six fcc metals considered (a) and in the Ag, Au and Pt atoms at the interface when combined with each of the six bcc metals considered (b).

black line) with that in an atom in the middle of the same block (dashed red line). It can be observed that the profile of the d band in the inner layer approximately stays constant regardless the metal Ag (W) is combined with; conversely, it changes quite drastically at the interface, depending on the metal at the other side. Finally, we noticed a tendency of the fcc crystal to modify its lattice parameter in the plane parallel to the interface (with $a_{\rm fcc}/\sqrt{2}$ increasing by up to 0.7 Å, see Fig. S4 of the Supporting Information) more than in bcc (for which $a_{\rm bcc}$ tends to remain unaffected, with an average variation of 0.01 Å).

4. Conclusions

In summary, we have demonstrated a novel way of computing interface energies. Our method was constructed as an extension of the Fiorentini method, which was developed for calculating surface energies. We studied fcc-bcc metal-metal interfaces in the (100) orientation. We found a dependence of the interface energy on the difference between the work functions of the two metals as well as the total number of d electrons per unit

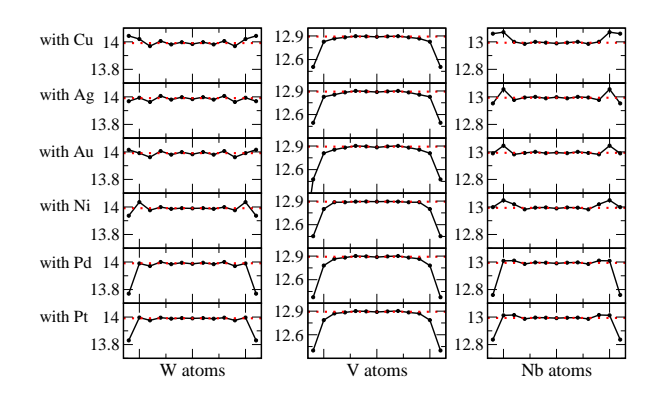


Figure 5: Löwdin charges for all atoms in W, V and Nb when interfaced with each of the six fcc metals considered. The horizontal red dotted line indicates the bulk value.

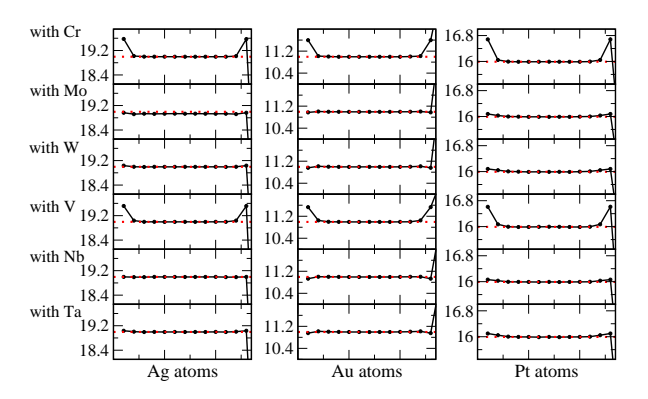


Figure 6: Löwdin charges for all atoms in Ag, Au and Pt when interfaced with each of the six bcc metals considered. The horizontal red dotted line indicates the bulk value.

cell. We believe that such relationships between interface energies and bulk properties can be useful for selecting materials and optimizing their adhesion. Interestingly, the trend of the interface energy is reflected in the position of the d band in the bcc metal with respect to the common interface Fermi level, whereas the same does not apply for its fcc counterpart. For the systems with the lowest interface energies, Löwdin charges show a clear sign of charge depletion in the bcc metal at the boundaries. The reliable first-principles prediction of surface and interface energetics is a longstanding challenge of significant technological relevance. The efficient methodology proposed and trends revealed in this work now provide a new route to achieving this for metals. It remains to be seen whether the energetic effects of complicating factors such as strain and reorganisation, chemical

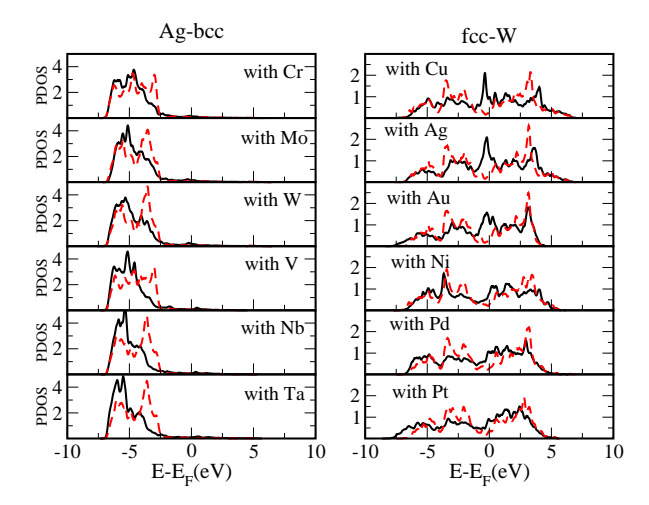


Figure 7: Projected density of state (PDOS) in the atom at the interface (solid black line) and in a inner layer (red dashed line) in Ag (left) and W (right) when combined with each of the bcc (fcc) metals considered. All energetics position are evaluated with respect to the global Fermi level of the interface.

bonding effects such as at oxide interfaces, and the emergence of interface magnetization and polarization are also amenable at least semi-quantitatively to simple bulk descriptors. This is a promising avenue for future investigation.

Acknowledgements

This publication has culminated from research supported in part by a research grant from Science Foundation Ireland (SFI) under Grant Number SFI/12/RC/2278. LAZ acknowledges support from the Spanish MINECO through the grant MAT2014-58982-JIN. All calculations were performed on the Boyle cluster maintained by the Trinity Centre for High Performance Computing. This cluster was funded by the European Research Council under the Quest project. The authors would like to thank John Donegan and David McCloskey of Trinity College Dublin for helpful discussions.

References

References

[1] A. Hung, I. Yarovsky, J. Muscat, S. Russo, I. Snook, R. Watts, First-principles study of metallic iron interfaces, Surf. Sci. 501 (3) (2002) 261–269. doi:https://doi.org/10.1016/S0039-6028(01)01762-9.

- [2] D. Jiang, J. Long, M. Cai, Y. Lin, P. Fan, H. Zhang, M. Zhong, Femtosecond laser fabricated micro/nano interface structures toward enhanced bonding strength and heat transfer capability of w/cu joining, Mater. Des. 114 (Supplement C) (2017) 185 – 193. doi:https://doi.org/10.1016/j.matdes.2016.11.094.
- [3] M. H. Athar, B. Tolaminejad, Weldability window and the effect of interface morphology on the properties of al/cu/al laminated composites fabricated by explosive welding, Mater. Des. 86 (Supplement C) (2015) 516 525. doi:https://doi.org/10.1016/j.matdes.2015.07.114.
- [4] T. J. Raeker, A. E. DePristo, The definition and calculation of interfacial energies for thin films, Surf. Sci. 310 (1-3) (1994) 337-346. doi:https://doi.org/10.1016/0039-6028(94)91397-8
- [5] B. Sonderegger, E. Kozeschnik, Generalized nearestneighbor broken-bond analysis of randomly oriented coherent interfaces in multicomponent fcc and bcc structures, Metall. Mater. Trans. A 40 (3) (2009) 499–510. doi:10.1007/s11661-008-9752-6.
- [6] K. Palotás, I. Bakó, L. Bugyi, Structural, electronic and adsorption properties of rh (111)/mo (110) bimetallic catalyst: A dft study, Appl. Surf. Sci. 389 (2016) 1094–1103. doi:https://doi.org/10.1016/j.apsusc.2016.08.020.
- [7] G. Feldbauer, M. Wolloch, P. O. Bedolla, P. Mohn, J. Redinger, A. Vernes, Adhesion and material transfer between contacting al and tin surfaces from first principles, Phys. Rev. B 91 (16) (2015) 165413. doi:https://doi.org/10.1103/PhysRevB.91.165413.
- [8] S. Lu, H. Zhang, Q.-M. Hu, M. P. Punkkinen, B. Johansson, L. Vitos, Magnetic effect on the interfacial energy of the ni (1 1 1)/cr (1 1 0) interface, J. Phys-Condens. Mat 26 (35) (2014) 355001. doi:https://doi.org/10.1088/0953-8984/26/35/355001.
- [9] W.-S. Jung, S.-H. Chung, Ab initio calculation of interfacial energies between transition metal carbides and fcc iron, Model. Simul. Mater. Sc. 18 (7) (2010) 075008. doi:https://doi.org/10.1088/0965-0393/18/7/075008.
- [10] H. Sawada, S. Taniguchi, K. Kawakami, T. Ozaki, First-principles study of interface structure and energy of fe/nbc, Model. Simul. Mater. Sc. 21 (4) (2013) 045012. doi:https://doi.org/10.1088/0965-0393/21/4/045012.
- [11] P. Haney, D. Waldron, R. Duine, A. Núñez, H. Guo, A. MacDonald, Ab initio giant magnetoresistance and current-induced torques in cr/ au/ cr multilayers, Phys. Rev. B 75 (17) (2007) 174428. doi:https://doi.org/10.1103/PhysRevB.75.174428.
- [12] X. W. Guan, X. M. Cheng, T. Huang, S. Wang, K. H. Xue, X. S. Miao, Effect of metal-tometal interface states on the electric-field modified magnetic anisotropy in mgo/fe/non-magnetic metal, Journal of Applied Physics 119 (13) (2016) 133905. arXiv:https://doi.org/10.1063/1.4945025, doi:10.1063/1.4945025.
 - URL https://doi.org/10.1063/1.4945025
- [13] C. Fu, A. J. Freeman, T. Oguchi, Prediction of strongly enhanced two-dimensional ferromagnetic moments on metallic overlayers, interfaces, and superlattices, Phys. Rev. Lett. 54 (25) (1985) 2700. doi:https://doi.org/10.1103/PhysRevLett.54.2700.
- [14] Y. Linghu, X. Wu, R. Wang, W. Li, Q. Liu, The adhesive properties of coherent and semicoherent nial/v interfaces within the peierls-nabarro model, Crystals 6 (4)

- (2016) 32. doi:10.3390/cryst6040032.
- [15] N.-Y. Park, J.-H. Choi, P.-R. Cha, W.-S. Jung, S.-H. Chung, S.-C. Lee, First-principles study of the interfaces between fe and transition metal carbides, J. Phys. Chem. C 117 (1) (2012) 187–193. doi:10.1021/jp306859n.
- [16] T. Li, T. Liu, H. Wei, S. Hussain, B. Miao, W. Zeng, X. Peng, F. Pan, Atomic and electronic structure of the tin/mgo interface from first principles, Comp. Mater. Sci. 105 (2015) 83-89. doi:https://doi.org/10.1016/j.commatsci.2015.04.005.
- [17] Energetic analysis of he and monovacancies in cu/w metallic interfaces, Mater. Des. 91 (Supplement C) (2016) 171 179. doi:https://doi.org/10.1016/j.matdes.2015.11.097.
- [18] S. Wang, H. Ye, Theoretical studies of solid-solid interfaces, Curr. Opin. Solid St. M. 10 (1) (2006) 26-32. doi:https://doi.org/10.1016/j.cossms.2006.06.001
- [19] S. Ziaei, Q. Wu, M. A. Zikry, Orientation relationships between coherent interfaces in hcpfcc systems subjected to high strain-rate deformation and fracture modes, Journal of Materials Research 30 (15) (2015) 23482359. doi:10.1557/jmr.2015.207.
- [20] S. Weng, H. Ning, N. Hu, C. Yan, T. Fu, X. Peng, S. Fu, J. Zhang, C. Xu, D. Sun, Y. Liu, L. Wu, Strengthening effects of twin interface in cu/ni multilayer thin films a molecular dynamics study, Mater. Des. 111 (Supplement C) (2016) 1 - 8. doi:https://doi.org/10.1016/j.matdes.2016.08.069.
- [21] J. M. Jung, J. G. Kim, M. I. Latypov, H. S. Kim, Effect of the interfacial condition on the microtexture near the interface of al/cu composites during multi-pass caliber rolling, Mater. Des. 82 (Supplement C) (2015) 28 – 36. doi:https://doi.org/10.1016/j.matdes.2015.05.025.
- [22] L. Martin, G. Vallverdu, H. Martinez, F. Le Cras, I. Baraille, First principles calculations of solid-solid interfaces: an application to conversion materials for lithium-ion batteries, J. Mater. Chem. 22 (41) (2012) 22063–22071. doi:10.1039/C2JM35078E.
- [23] A. Martins, M. de Campos, Energy of ni/ni 3 al interface: A temperature-dependent theoretical study, Mater. Lett. 83 (2012) 100-103. doi:https://doi.org/10.1016/j.matlet.2012.05.057
- [24] S. Nazir, J. Cheng, M. Behtash, J. Luo, K. Yang, Interface energetics and charge carrier density amplification by sn-doping in laalo3/srtio3 heterostructure, ACS Appl. Mater. Interfaces 7 (26) (2015) 14294–14302. doi:10.1021/acsami.5b02770.
- [25] R. Li, S. Lu, D. Kim, S. Schnecker, J. Zhao, S. K. Kwon, L. Vitos, Stacking fault energy of face-centered cubic metals: thermodynamic and ab initio approaches, Journal of Physics: Condensed Matter 28 (39) (2016) 395001.
- [26] L. Hu, Y. Xue, F. Shi, Intermetallic formation and mechanical properties of ni-ti diffusion couples, Mater. Des. 130 (Supplement C) (2017) 175 – 182. doi:https://doi.org/10.1016/j.matdes.2017.05.055
- [27] F. Gautier, A. Llois, Adhesion of transition metals: energies and thin film deposition: An electronic approach, Surf. Sci. 245 (1-2) (1991) 191–206. doi:https://doi.org/10.1016/0039-6028(91)90478-B.
- [28] D. H. Fors, S. A. Johansson, M. V. Petisme, G. Wahnström, Theoretical investigation of moderate misfit and interface energetics in the fe/vn system, Comp. Mater. Sci. 50 (2) (2010) 550–559.

- doi:https://doi.org/10.1016/j.commatsci.2010.09.018.
- [29] S. Lu, Q.-M. Hu, M. P. Punkkinen, B. Johansson, L. Vitos, First-principles study of fcc-ag/bcc-fe interfaces, Phys. Rev. B 87 (22) (2013) 224104. doi:https://doi.org/10.1103/PhysRevB.87.224104.
- [30] K. Zhao, D. Chen, D. Li, First principles study of interface structure and electronic property of au/srtio 3 (001), Comp. Mater. Sci. 50 (1) (2010) 98-104. doi:https://doi.org/10.1016/j.commatsci.2010.07.012.
- [31] V. Fiorentini, M. Methfessel, Extracting convergent surface energies from slab calculations, J. Phys-Condens. Mat 8 (36) (1996) 6525. doi:https://doi.org/10.1088/0953-8984/8/36/005.
- [32] N. E. Singh-Miller, N. Marzari, Surface energies, work functions, and surface relaxations of low-index metallic surfaces from first principles, Phys. Rev. B 80 (23) (2009) 235407. doi:https://doi.org/10.1103/PhysRevB.80.235407.
- [33] G. Allan, M. Lannoo, L. Dobrzynski, Simple self-consistent theory of adhesion at a bimetallic interface, Philos. Mag. 30 (1) (1974) 33-45. doi:http://dx.doi.org/10.1080/14786439808206531.
- [34] P. Giannozzi, S. Baroni, N. Bonini, M. Calandra, R. Car, C. Cavazzoni, D. Ceresoli, G. L. Chiarotti, M. Cococcioni, I. Dabo, A. D. Corso, S. de Gironcoli, S. Fabris, G. Fratesi, R. Gebauer, U. Gerstmann, C. Gougoussis, A. Kokalj, M. Lazzeri, L. Martin-Samos, N. Marzari, F. Mauri, R. Mazzarello, S. Paolini, A. Pasquarello, L. Paulatto, C. Sbraccia, S. Scandolo, G. Sclauzero, A. PSeitsonen, A. Smogunov, P. Umari, R. M. Wentzcovitch, Quantum espresso: a modular and open-source software project for quantum simulations of materials, J. Phys-Condens. Mat 21 (39) (2009) 395502. http://stacks.iop.org/0953-8984/21/i=39/a=395502.
- [35] R. Pérez, P. Gumbsch, An ab initio study of the cleavage anisotropy in silicon, Acta Materialia 48 (18) (2000) 4517–4530. doi:https://doi.org/10.1016/S1359-6454(00)00238-X.
- [36] H. J. Monkhorst, J. D. Pack, Special points for brillouin-zone integrations, Phys. Rev.B 13 (1976) 5188. doi:https://doi.org/10.1103/PhysRevB.13.5188.
- [37] K. F. Garrity, J. W. Bennett, K. M. Rabe, D. Vanderbilt, https://www.physics.rutgers.edu/gbrv/.
- [38] J. Das, S. Biswas, A. K. Kundu, S. Narasimhan, K. S. Menon, Structure of cr monolayer on ag (001): A buried two-dimensional c (2× 2) antiferromagnet, Phys. Rev. B 91 (12) (2015) 125435. doi:https://doi.org/10.1103/PhysRevB.91.125435.
- [39] H. Röder, R. Schuster, H. Brune, K. Kern, Monolayer-confined mixing at the ag-pt (111) interface, Phys. Rev. Lett. 71 (13) (1993) 2086. doi:https://doi.org/10.1103/PhysRevLett.71.2086.
- [40] J. K. Nørskov, F. Abild-Pedersen, F. Studt, T. Bli-gaard, Density functional theory in surface chemistry and catalysis, Proceedings of the National Academy of Sciences 108 (3) (2011) 937–943. doi:doi:10.1073/pnas.1006652108.
- [41] W. Tang, G. Henkelman, Charge redistribution in core-shell nanoparticles to promote oxygen reduction, J. Chem. phys. 130 (19) (2009) 194504. doi:doi:http://dx.doi.org/10.1063/1.3134684.
- [42] D. Holec, P. H. Mayrhofer, Surface energies of aln allotropes from first principles, Scripta Mater. 67 (9) (2012) 760-762. doi:https://doi.org/10.1016/j.scriptamat.2012.07.027.

[43] J. Wang, S.-Q. Wang, Surface energy and work function of fcc and bcc crystals: Density functional study, Surf. Sci. 630 (2014) 216–224. doi:https://doi.org/10.1016/j.susc.2014.08.017.